

## Article

# Highly-Efficient and Visible Light Photocatalytical Degradation of Organic Pollutants Using TiO<sub>2</sub>-Loaded on Low-Cost Biomass Husk

Yuan Li <sup>1</sup>, Xirong Lin <sup>2</sup>, Zhanpeng Li <sup>3,\*</sup> and Jinyun Liu <sup>4,5,\*</sup> <sup>1</sup> Sichuan Vocational and Technical College, Suining 629000, China<sup>2</sup> National Key Laboratory of Science and Technology on Micro/Nano Fabrication, Department of Micro/Nano-Electronics, Shanghai Jiao Tong University, Shanghai 200240, China<sup>3</sup> Nanjing Noland Environmental Engineering Technology Co., Ltd., Nanjing 211215, China<sup>4</sup> Key Laboratory of Functional Molecular Solids, Ministry of Education, College of Chemistry and Materials Science, Anhui Normal University, Wuhu 241002, China<sup>5</sup> Anhui Key Laboratory of Molecule-Based Materials, College of Chemistry and Materials Science, Anhui Normal University, Wuhu 241002, China

\* Correspondence: lizhanp007@163.com (Z.L.); jyliu@iim.ac.cn (J.L.)

**Abstract:** A composite composing of TiO<sub>2</sub> nanoparticles load on biomass rice husk (RH) is developed by directly growing TiO<sub>2</sub> nanoparticles on RH. The in-situ growth of the nanocrystals on RH is achieved by a low-cost and one-step homogeneous precipitation. Rapid hydrolysis proceeds at 90 °C by using ammonium fluotitanate and urea to facilitate the selective growth of TiO<sub>2</sub>. The method provides an easy access to the TiO<sub>2</sub>-RH composite with a strong interaction between TiO<sub>2</sub> nanoparticles and the underlying RH. The structure and composition of TiO<sub>2</sub>-RH are characterized by using X-ray diffraction, X-ray photoelectron spectroscopy, Fourier-transform infrared spectroscopy, and UV-vis absorption spectroscopy. TiO<sub>2</sub> nanoparticles-RH exhibits a good photocatalytic degradation of methyl orange. The results show that 92% of methyl orange (20 mg L<sup>-1</sup>) can be degraded within three hours in visible light. The catalytic activity of the composite is not reduced after 6 cycles, and it still reaches 81% after 6 cycles. The enhanced performance is ascribed to the suitable particle size the good dispersibility. It is expected that the high photocatalytical performance and the cost-effective composite presented here will inspire the development of other high-performance photocatalysts.

**Keywords:** TiO<sub>2</sub>; rice husk; photodegradation; methyl orange; ecological restoration



**Citation:** Li, Y.; Lin, X.; Li, Z.; Liu, J. Highly-Efficient and Visible Light Photocatalytical Degradation of Organic Pollutants Using TiO<sub>2</sub>-Loaded on Low-Cost Biomass Husk. *Materials* **2022**, *15*, 8671. <https://doi.org/10.3390/ma15238671>

Academic Editor: Klaus Stowe

Received: 9 November 2022

Accepted: 2 December 2022

Published: 5 December 2022

**Publisher's Note:** MDPI stays neutral with regard to jurisdictional claims in published maps and institutional affiliations.



**Copyright:** © 2022 by the authors. Licensee MDPI, Basel, Switzerland. This article is an open access article distributed under the terms and conditions of the Creative Commons Attribution (CC BY) license (<https://creativecommons.org/licenses/by/4.0/>).

## 1. Introduction

Photodegradation of organic pollutants has received many interests during the past decades [1]. Titanium dioxide is distinguished and widely studied as a semiconductor photocatalysis [2,3]. It has been considered a promising catalyst because of its non-toxicity, cheapness, stability and high reactivity [4], and it has been used for removing environmental pollutants in air or water [5,6]. In recent years, organic/inorganic composites are used as catalysts, sensors, etc [7–9]. Some reports display that the TiO<sub>2</sub>-based composites show improved catalytic activities [10–13].

Methyl orange (MO) is a common acid-anionic mono-azo dye which contains an azo group (-N=N-). MO is used widely in printing and dyeing industries. The release of MO is harmful to the environment. As a result, the removal of MO in the industrial waste water has been of the most important tasks. As a represented azo dye, MO has been employed as a simulated target for photocatalytical measurements [14].

Biomass waste is a kind of cheap and easily available natural organic resource. Rice husk (RH) is composed of cellulose (34–46%), pentose (21–22%), lignin (9–20%), and protein (2–3%), which is an abundant agro-industrial residue [15,16]. However, there is still a considerable amount that cannot be used rationally, causing serious environmental

problems. RH with tubular structure has a large specific surface area, rich resources, ideal chemical stability and robust strength. These characteristics enable RH to be used to remove heavy metal ions in aqueous solutions [17,18]. There is a layer of SiO<sub>2</sub> on the outer surface of rice husk as a protective film for natural RH [19]. By using the alkali treatment, SiO<sub>2</sub> can be removed, so that some functional groups could be exposed on the surface of RH. In addition, the ester bond between cellulose and lignin can be opened, and part of the cellulose and lignin can be dissolved to increase the loading of TiO<sub>2</sub>, and thus, enhancing the catalytic activity of TiO<sub>2</sub>-RH composite.

Despite a good photocatalytic activity of granular TiO<sub>2</sub> nanoparticles, their recycling and reuse limit their application in water treatment, leading to considerable loss [20–22]. Due to relatively mild catalytic conditions, moderate catalytic activity, environmental friendliness, and relatively low biological toxicity, TiO<sub>2</sub> photocatalyst has become an ideal choice to remove organic pollutants in air and water [23,24]. Although TiO<sub>2</sub> nanoparticles have high scientific research value, the size of their particles limits their practical application in water treatment. Considering this, it is relatively difficult to recover and reuse them, and the synthesis cost is high. Moreover, the complicated environment in water is easy to interfere with the surface properties of TiO<sub>2</sub>, which limits their applications in water treatment [25].

In order to enhance the reuse capability of TiO<sub>2</sub>, RH is used as a substrate to load TiO<sub>2</sub>. The RH loaded with TiO<sub>2</sub> nanoparticles can contact well with pollutants in water and achieve a good photocatalytic activity of the TiO<sub>2</sub>-RH composite. Here, TiO<sub>2</sub>-RH composite is prepared through a co-precipitation approach, which is used to decompose MO in visible light. The developed preparation method and the prepared photocatalyst would possess the following features: (i) The preparation method is quite simple. A low-temperature one-step approach for preparing anatase TiO<sub>2</sub> reduces the preparation cost, which is significant for potential applications. (ii) TiO<sub>2</sub> photocatalyst has many applications in the treatment of exhaust gases; however, it is restricted due to the potential biotoxicity when the particle size is non-ideal. In our study, the particle size is able to be controlled easily at around 100 to 300 nm which has a low biotoxicity, and it is beneficial for real use. (iii) The TiO<sub>2</sub>-RH developed here displays a high photocatalytic performance due to the suitable particle size the good dispersibility. On the basis of an optimized amount of RH and the cycling experiments on the TiO<sub>2</sub>-RH photocatalyst, it maintains a high catalytic performance after six rounds of repeated degradation, indicating a potential commercializing value. Considering some previous reports [26], the TiO<sub>2</sub>-RH composite presented here is able to degrade 92% of methyl orange (20 mg L<sup>-1</sup>) within three hours in visible light, which is competitive compared to some other photocatalysts.

## 2. Experimental

### 2.1. Preparation of Composite

RH was purchased from Nanjing, China. (NH<sub>4</sub>)<sub>2</sub>TiF<sub>6</sub> (analytical grade) was obtained from Aladdin industrial Co., Ltd. (HongKong, China). NaOH, CO(NH<sub>2</sub>)<sub>2</sub> and MO (analytical grade) were obtained from Tianjing Kemiou Chemical Reagent Co., Ltd. After being broken and sieved, the RH was added in to a 0.5 mol L<sup>-1</sup> of NaOH solution. The solution was kept at 120 °C for 8 h. Then, RH was washed to neutral, then dried at 80 °C. A series of amounts of RH were added to the (NH<sub>4</sub>)<sub>2</sub>TiF<sub>6</sub> and CO(NH<sub>2</sub>)<sub>2</sub> solutions with stirring. The mixture was heated to 90 °C under stirring for 60 min. The final product was collected by centrifuge, washed with deionized water, and then dried at 80 °C. Samples with different contents of RH (0.5, 1.0, 1.5, 2.0, and 2.5 g) were prepared to investigate the effect of RH on the structure and photocatalytic performance. For example, TiO<sub>2</sub>-2RH represents 2 g of RH was added to load with TiO<sub>2</sub> nanoparticles.

### 2.2. Characterization

The prepared TiO<sub>2</sub>-RH was characterized by a Tongda TD-3500 X-ray powder diffractometer (XRD, Tonda S&T Co., Ltd., Dandong, China), field emission scanning electron

microscopy (FE-SEM, FEI company, USA), Hitachi S4800 scanning-electron microscope (Hitachi Company, Japan), Thermo Scientific Nicolet Fourier-transform infrared spectra (FTIR, Thermo Scientific Company, USA), and Kratos XSAM X-ray photoelectron spectra (XPS, Kratos Company, Manchester, England). In addition, UV-Vis spectra were obtained using a TU-1901 spectrophotometer (Dingnuo Co., Ltd., Shanghai, China).

### 2.3. Photocatalytic Evaluation

To investigate the photocatalytic activity of the  $\text{TiO}_2$ -RH, MO was used in a circulating water-cooling beaker with magnetic stirring. Photocatalysts (100 mg) were added in 100 mL of MO solution ( $20 \text{ mg L}^{-1}$ ) and stirred for 20 min before irradiation. Samples were taken at 30 min intervals during degradation. A 350 W high pressure xenon lamp, which emits a similar spectrum as sun, was used as the visible light source, which was positioned 20 cm away from circulating water-cooling beaker. The concentration of MO was measured at 464 nm using spectrophotometer.

## 3. Results and Discussion

The XRD patterns of the pure  $\text{TiO}_2$  and  $\text{TiO}_2$ -2RH are presented in Figure 1. According to the diffraction peaks of typical anatase  $\text{TiO}_2$  (JCPDS card No. 01-071-1166), the  $\text{TiO}_2$  without RH shows an anatase phase of titanium dioxide. The diffraction peak of  $\text{TiO}_2$ -2RH at  $22.5^\circ$  in the sample is caused by cellulose in the synthesized material [11–13]. The characteristic peak of  $\text{TiO}_2$  is not observed in the sample of  $\text{TiO}_2$ -2RH, probably because the characteristic peak of  $\text{TiO}_2$  is covered by the signals of RH [27].

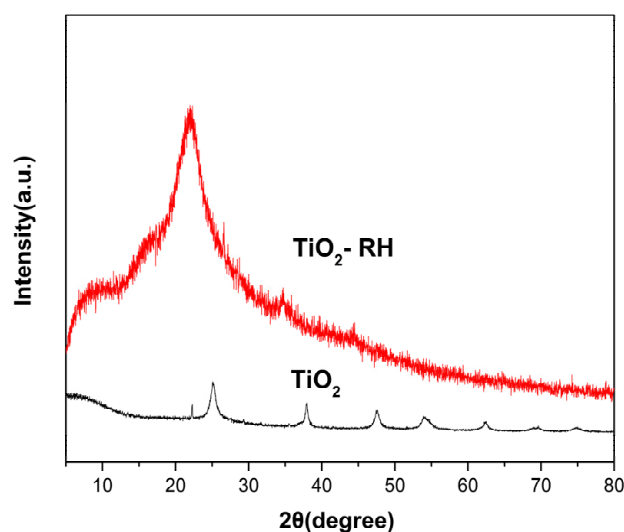
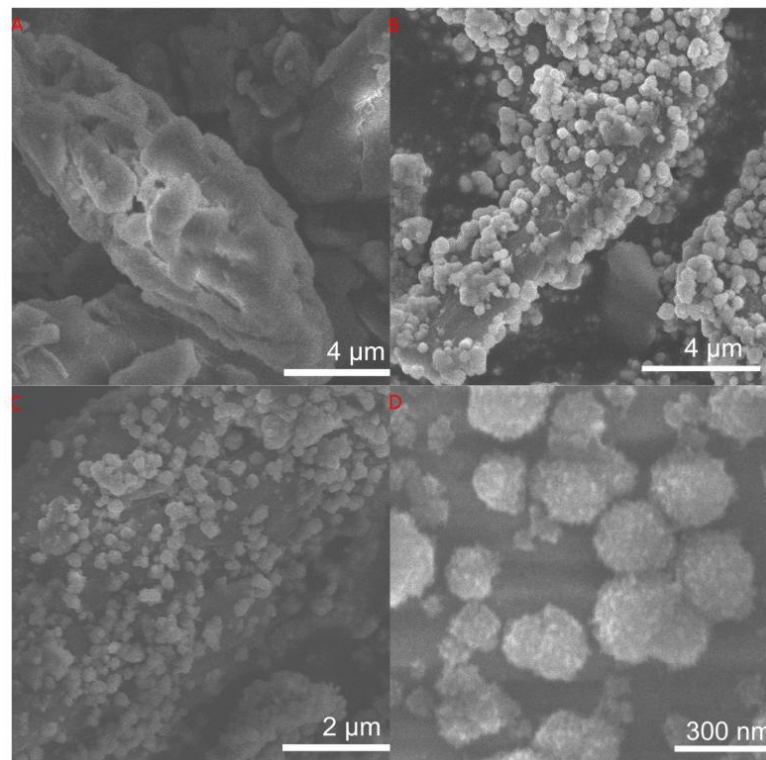


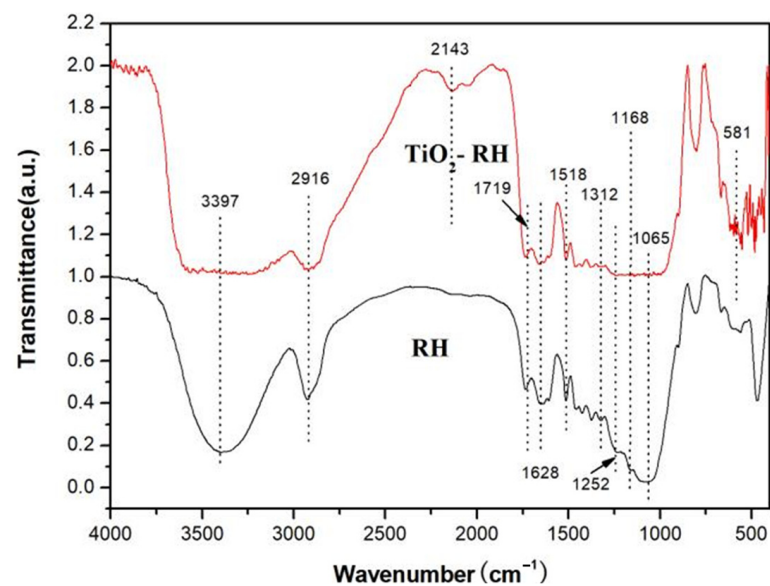
Figure 1. XRD patterns of  $\text{TiO}_2$  and  $\text{TiO}_2$ -RH.

Figure 2 displays the SEM photographs of RH and  $\text{TiO}_2$ -RH composite. The  $\text{TiO}_2$ -RH shows highly dispersed submicron-scale anatase  $\text{TiO}_2$  spheres with a layered structure. Each  $\text{TiO}_2$  microsphere has a hierarchical structure, indicating that the microsphere contains several  $\text{TiO}_2$  nanoparticles. The special structure of  $\text{TiO}_2$  microspheres indicates that it is formed by the aggregation of  $\text{TiO}_2$  nanoparticles on RH. SEM images show that dense  $\text{TiO}_2$  nanocrystals are assembled on the RH surface.  $\text{TiO}_2$  nanoparticles remain on the surface of the RH even under prolonged sonication, indicating a robust structure. The prepared  $\text{TiO}_2$ -RH composite is submicron, and the catalyst can be separated from the degraded object solution by simple filtration after the photocatalytic reactions. In Figure 2D, the SEM images shows that the particle size is between 100–300 nm, which is well controllable by changing the reaction time [23,24].



**Figure 2.** SEM images of the (A) RH and (B–D) TiO<sub>2</sub>-2RH.

In Figure 3, FTIR spectra of RH and TiO<sub>2</sub>-RH composite are presented. Vibration absorption band of TiO<sub>2</sub>-RH composite between 1400 and 450 cm<sup>-1</sup> belongs to characteristic mode of TiO<sub>2</sub>. The bands at 610 and 1390 cm<sup>-1</sup> are ascribed to Ti–O and Ti–O–Ti stretching, respectively [11–13]. Strong –OH stretching (3300–3500 cm<sup>-1</sup>) in TiO<sub>2</sub> and TiO<sub>2</sub>-RH composite may be due to the adsorbed water [12]. FT-IR spectrum of RH presents a vibrational band at 2916 cm<sup>-1</sup>, which is assigned to C–H stretching; while the band at 1628 cm<sup>-1</sup> is indexed to C=C stretching. The band between 1387–1016 cm<sup>-1</sup> may be caused by C–O stretching and C=C bending, and such vibrational peaks mostly belong to cellulose, lignin, and biopolymers [11].



**Figure 3.** FTIR spectra of RH and TiO<sub>2</sub>-RH.

In Figure 4, both the specific surface area and pore volume of the synthesized TiO<sub>2</sub>-RH composite increase, while the average pore-size decreases. In other words, the improvement of the catalytic performance of the composite is also related to the increase in the specific surface area, as shown in Table 1.

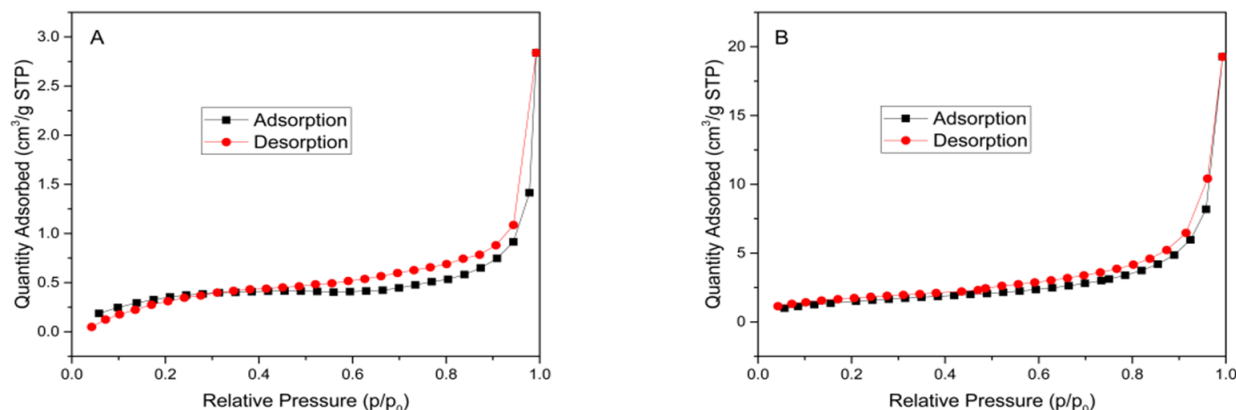


**Figure 4.** Adsorption-desorption profiles of (A) RH and (B) TiO<sub>2</sub>-RH.

**Table 1.** Surface parameters of RH and TiO<sub>2</sub>-RH.

Sample	Specific Surface Area (m <sup>2</sup> g <sup>-1</sup> )	Pore Volume (cm <sup>3</sup> g <sup>-1</sup> )	Average Pore Diameter (nm)
RH	1.0542	0.004392	11.2855
TiO <sub>2</sub> -RH	4.9642	0.029811	6.5425

In addition, we conducted XPS measurements on the TiO<sub>2</sub>-RH composite. In Figure 5, it can be seen that there are mainly titanium, carbon, oxygen, iron, and other elements in the composite. In the Ti 2p spectrum, the peaks at 458.9 and 464.2 eV correspond to Ti 2p<sub>3/2</sub> and Ti 2p<sub>1/2</sub>, respectively, which further verifies the existence of Ti<sup>4+</sup> oxidation state in TiO<sub>2</sub>-RH. According to Figure 5C, C-O-Ti exists in TiO<sub>2</sub>-RH composite, which proves that TiO<sub>2</sub> crystal and RH are combined in the form of chemical bond. The two peaks of the O 1s at 530.2 and 532.4 eV correspond to lattice oxygen and C-O in RH. Figure 5E shows the presence of an oxide of Fe, which may be introduced by the shredder during rice-husk shredding [27,28].

Figure 6A shows the UV-vis absorption spectrum of TiO<sub>2</sub>-RH composite. As expected, the characteristic peak of TiO<sub>2</sub> nanocrystals is around 400 nm, and there is almost no absorption of light higher than 400 nm. However, it is interesting to note that the TiO<sub>2</sub>-RH composite exhibits an unusual UV-visible absorption when the TiO<sub>2</sub> is loaded on RH. The UV-vis absorption peak of the TiO<sub>2</sub>-RH composite has a redshift relative to the TiO<sub>2</sub> nanoparticles. Moreover, the amount of RH also affects the optical properties of TiO<sub>2</sub>-RH. Wavelength of light absorbed by the composite almost covers the entire UV-visible region. This phenomenon is consistent with the optical properties of carbon-doped anatase TiO<sub>2</sub>. TiO<sub>2</sub>-RH composite can absorb more light than single TiO<sub>2</sub> nanoparticles, indicating that the composite would be able to improve the absorption of visible light, which may also change the process of generating electron-hole pairs in visible light [13]. On the basis of these mechanism, this unique structure of TiO<sub>2</sub>-RH composite exhibits an improved photocatalytic activity in visible light. Figure 6B shows that the band-gap energy of TiO<sub>2</sub>-RH composite is lower than that of pure TiO<sub>2</sub>, which may be related to the combination of TiO<sub>2</sub> and rice husk in the composite system [25,28].

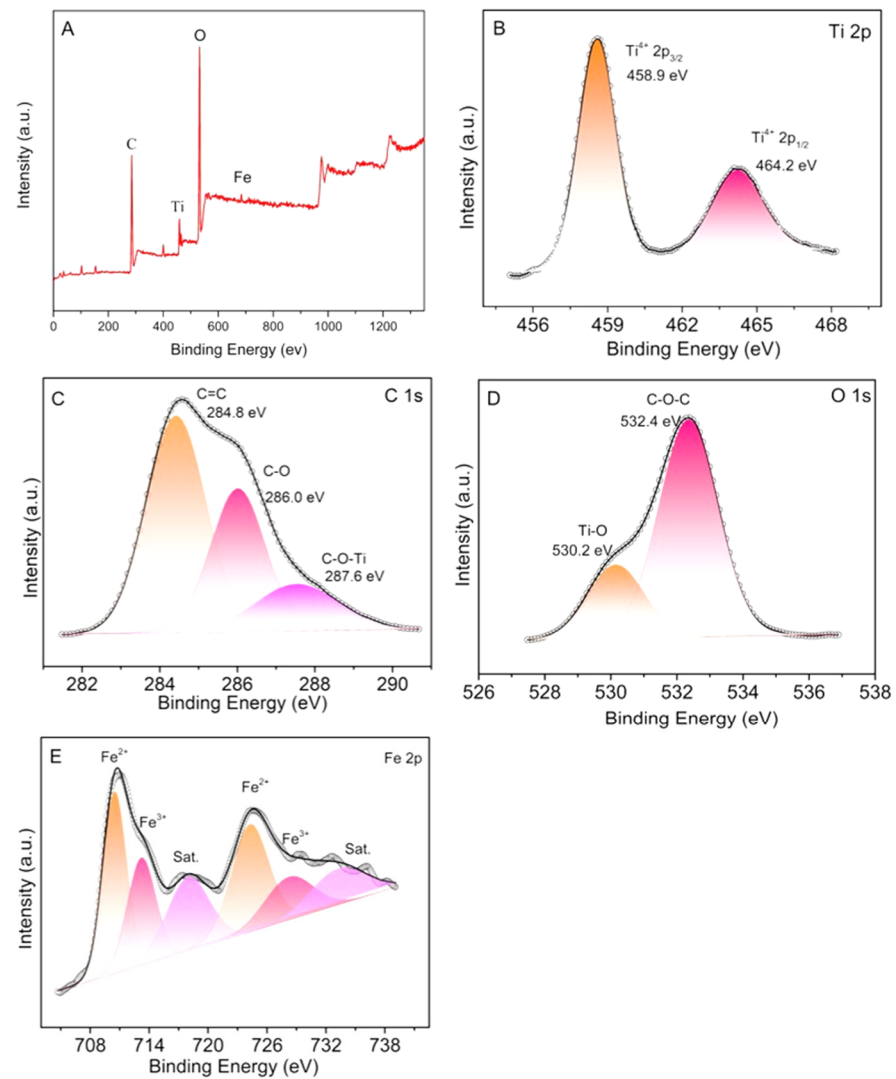


**Figure 5.** XPS spectra of the TiO<sub>2</sub>-RH composite: (A) Survey spectrum, (B) Ti 2p, (C) C 1s, (D) O 1s, and (E) Fe 2p.

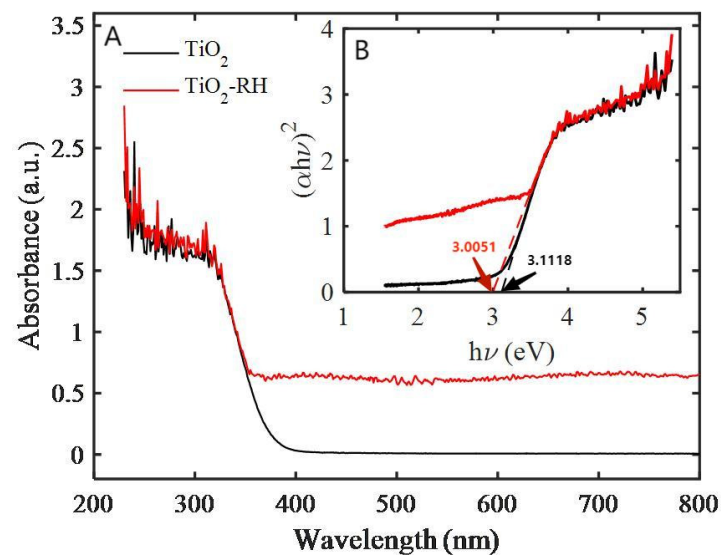


**Figure 6.** (A) UV-vis absorption spectra, (B) Tauc's profile for the band-gap determination.

The degradation of MO by  $\text{TiO}_2$  and  $\text{TiO}_2$ -RH composites under visible light was investigated, as displayed in Figure 7A.  $\text{TiO}_2$  without RH exhibits a weak photocatalytic activity and degradation rate of MO after 3 h is about 43%. Pure RH displays no capability of photodegradation. In contrast, for the  $\text{TiO}_2$ -RH samples with RH = 0.5, 1.0, 1.5, 2.0, and 2.5 g, the degradation rates are 69.4%, 87.4%, 86.2, 92.6%, and 90.3%, respectively. With a small amount of RH, the low catalytic activity is ascribed to the accumulation of  $\text{TiO}_2$  nanoparticles on the surface of RH, which are not well dispersed. Depending on the increase of RH content, the catalytic activity is improved. However, if the amount of RH increases further, the decrease in photocatalytic activity may be caused by the decrease in  $\text{TiO}_2$  content in the composite. The catalytic performance of  $\text{TiO}_2$ -RH composite is improved compared with  $\text{TiO}_2$  under visible light; this may be because  $\text{TiO}_2$ -RH composite has a certain light absorption in visible light region, while  $\text{TiO}_2$  has very less absorption in visible light. As can be seen from the XPS spectrum, the existence of C-O-Ti bond in  $\text{TiO}_2$ -RH composite indicates that  $\text{TiO}_2$  and RH are combined by chemical bond, rather than van der Waals force, which is more conducive to the separation and transmission of electrons. With the increase of RH amount, the catalytic performance is enhanced, possibly because  $\text{TiO}_2$  is more dispersed on the RH surface rather than agglomeration. When the amount of RH reaches 2 g, the catalytic performance is the highest. If the amount increases continuously, the catalytic performance decreases, possibly because the amount of active  $\text{TiO}_2$  catalyst is reduced.  $\text{TiO}_2$  crystals synthesized by co-precipitate method are spherical in shape, and the binding with RH is in the form of C-O-Ti. Therefore, the key factor affecting the catalytic performance would be the effective dispersion of  $\text{TiO}_2$  on the surface of RH. In the prepared  $\text{TiO}_2$ -RH, it exhibits a reduced agglomeration, which enables a good catalytic performance compared to the pure  $\text{TiO}_2$  nanoparticles [29].

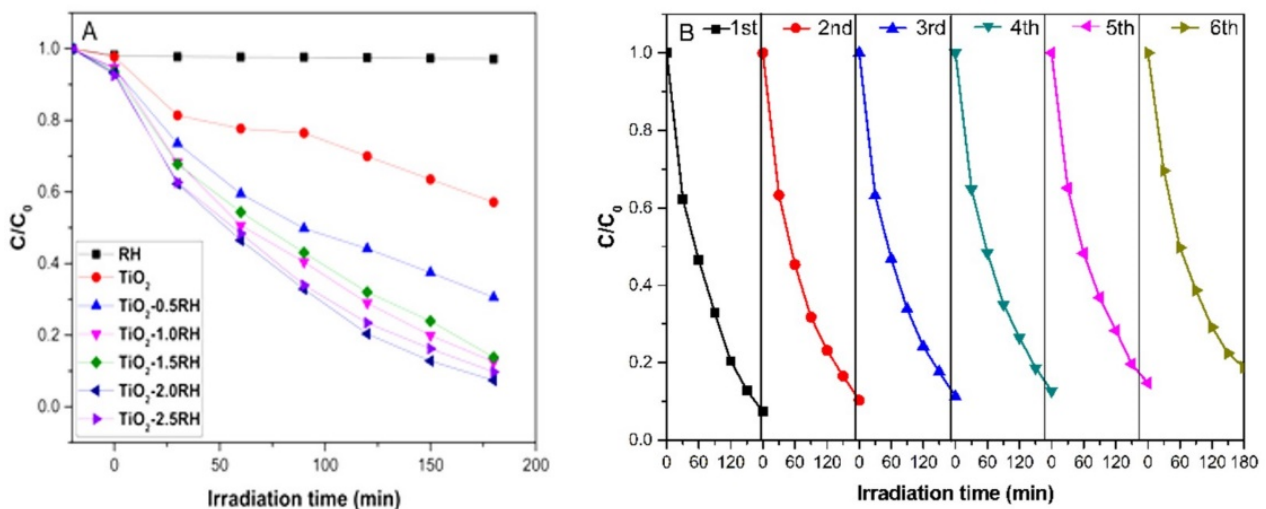


**Figure 7.** (A) Photodegradation kinetics of  $\text{TiO}_2$ -RH towards  $20 \text{ mg L}^{-1}$  MO solution in visible light. (B) Cycling photodegradation of MO by  $\text{TiO}_2$ -2RH under visible light.

Figure 7B shows  $\text{TiO}_2$ -2RH composite cyclically degrading MO ( $20 \text{ mg L}^{-1}$ ) in visible light for 180 min per cycle. The catalytic activity of the composite is not significantly reduced after 6 cycles, and it still reaches 81% after 6 cycles. The decrease in the activity of the photocatalyst may be due to the partial shedding of the loaded  $\text{TiO}_2$  nanoparticles.

#### 4. Conclusions

In summary, a composite based on RH loading with dense  $\text{TiO}_2$  nanoparticles is developed by a co-precipitation method. The developed preparation method is quite simple. Low-temperature one-step approach for preparing anatase  $\text{TiO}_2$  reduces the preparation cost, which is significant for potential applications.  $\text{TiO}_2$  photocatalyst has many applications in the treatment of exhaust gases; however, it is restricted due to the potential

biotoxicity when the particle-size is non-ideal. In our study, the particle-size is able to be controlled easily at around 100 to 300 nm which has been considered has a low biotoxicity for use. Moreover, the TiO<sub>2</sub>-RH developed here displays a high photocatalytic performance due to the suitable particle-size the good dispersibility. The composite shows a good potential in the photocatalytic degradation of MO in visible light. The results show that 92% of MO can be degraded within three hours in visible light. A good cycling photodegradation performance for six rounds is also achieved. It is expected that some other highly-efficient TiO<sub>2</sub> composite photocatalysts can also be obtained from agricultural biowastes, such as straw, wheat bran, corn cobs, and sawdust. This work converts agricultural biomass waste into a high-performance photocatalyst, and exhibits a promising application for in wastewater treatment. In addition, it is considered that the degradation efficiency of TiO<sub>2</sub> under visible light would be further improved by doping metal ions and introducing single-atom catalyst, which would be promising research directions.

**Author Contributions:** Methodology, Y.L.; validation, Z.L.; formal analysis, Y.L., X.L., Z.L. and J.L.; writing—original draft preparation, Y.L., X.L., Z.L. and J.L.; writing—review and editing, Z.L. and J.L.; supervision, Z.L. and J.L. All authors have read and agreed to the published version of the manuscript.

**Funding:** This research work was funded by the Key Research and Development Program of Wuhu (2022YF53) and the Foundation of Anhui Laboratory of Molecule-Based Materials (FZJ21012).

**Institutional Review Board Statement:** Not applicable.

**Informed Consent Statement:** Not applicable.

**Data Availability Statement:** Not applicable.

**Conflicts of Interest:** The authors declare no conflict of interest.

## References

1. Kaur, K.; Badru, R.; Singh, P.P.; Kaushal, S. Photodegradation of organic pollutants using heterojunctions: A review. *J. Environ. Chem. Eng.* **2020**, *8*, 103666.
2. AlAbdulaal, T.H.; Ganesh, V.; AlShadidi, M.; Hussien, M.S.A.; Bouzidi, A.; Algarni, H.; Zahran, H.Y.; Abdel-wahab, M.S.; Yahia, I.S.; Nasr, S. The auto-combustion method synthesized Eu<sub>2</sub>O<sub>3</sub>-ZnO nanostructured composites for electronic and photocatalytic applications. *Materials* **2022**, *15*, 3257. [[CrossRef](#)] [[PubMed](#)]
3. Gaya, U.I.; Abdullah, A.H. Heterogeneous photocatalytic degradation of organic contaminants over titanium dioxide: A review of fundamentals, progress and problems. *J. Photochem. Photobiol. C Photochem. Rev.* **2008**, *9*, 1–12. [[CrossRef](#)]
4. Hussien, M.S.A.; Bouzidi, A.; Abd-Rabboh, H.S.M.; Yahia, I.S.; Zahran, H.Y.; Abdel-wahab, M.S.; Alharbi, W.; Awwad, N.S.; Ibrahim, M.A. Fabrication and characterization of highly efficient as-synthesized WO<sub>3</sub>/graphitic-C<sub>3</sub>N<sub>4</sub> nanocomposite for photocatalytic degradation of organic compounds. *Materials* **2022**, *15*, 2482. [[CrossRef](#)] [[PubMed](#)]
5. Zhang, M.; Wang, Q.; Chen, C.; Zang, L.; Ma, W.; Zhao, J. Oxygen atom transfer in the photocatalytic oxidation of alcohols by TiO<sub>2</sub>: Oxygen isotope studies. *Angew. Chem. Int. Ed.* **2009**, *48*, 6081–6084. [[CrossRef](#)]
6. Ulfa, M.; Afif, H.A.; Saraswati, T.E.; Bahruji, H. Fast removal of methylene blue via adsorption-photodegradation on TiO<sub>2</sub>/SBA-15 synthesized by slow calcination. *Materials* **2022**, *15*, 5471. [[CrossRef](#)]
7. Dou, Q.Q.; Teng, C.P.; Ye, E.; Loh, X.J. Effective near-infrared photodynamic therapy assisted by upconversion nanoparticles conjugated with photosensitizers. *Int. J. Nanomed.* **2015**, *10*, 419–432.
8. Liao, G.Z.; Chen, S.; Quan, X.; Chen, H.; Zhang, Y.B. Photonic crystal coupled TiO<sub>2</sub>/ polymer hybrid for efficient photocatalysis under visible light irradiation. *Environ. Sci. Technol.* **2010**, *44*, 3481–3485. [[CrossRef](#)]
9. Nsib, M.F.; Hajji, F.; Mayoufifi, A.; Moussa, N.; Rayes, A.; Houas, A. In situ synthesis and characterization of TiO<sub>2</sub>/HPM cellulose hybrid material for the photocatalytic degradation of 4-NP under visible light. *Comptes Rendus Chim.* **2014**, *17*, 839–848. [[CrossRef](#)]
10. Virkutyte, J.; Jegatheesan, V.; Varma, R.S. Visible light activated TiO<sub>2</sub>/microcrystalline cellulose nanocatalyst to destroy organic contaminants in water. *Bioresour. Technol.* **2012**, *113*, 288–293. [[CrossRef](#)]
11. Hun, X.; Chen, Y.L.; Liu, P.; Qian, Q.R.; Luo, Y.J.; Cui, M.L.; Chen, Y.S.; Yang, D.P.; Chen, Q.H. Visible light-assisted efficient degradation of dye pollutants with biomass-supported TiO<sub>2</sub> hybrids. *Mater. Sci. Eng. C.* **2018**, *82*, 197–203.
12. Alghamdi, Y.G.; Balu, K.K.; Maqsood, A.M.; Sultan, A. Design and preparation of biomass-derived activated carbon loaded TiO<sub>2</sub> photocatalyst for photocatalytic degradation of reactive red 120 and ofloxacin. *Polymers* **2022**, *14*, 880. [[CrossRef](#)]
13. Alsaari, M. Biomass-derived active carbon (AC) modified TiO<sub>2</sub> photocatalyst for efficient photocatalytic reduction of chromium (VI) under visible light. *Arab. J. Chem.* **2021**, *14*, 103258. [[CrossRef](#)]

14. Darwish, A.A.A.; Rashad, M.; Al-Aoh, H.A. Methyl orange adsorption comparison on nanoparticles: Isotherm, kinetics, and thermodynamic studies. *Dyes Pigment.* **2019**, *160*, 563–571. [[CrossRef](#)]
15. Zou, Y.P.; Yang, T.K. Rice husk, rice husk ash and their applications. In *Rice Bran and Rice Bran Oil*; AOCs Press: Urbana, IL, USA, 2019; pp. 207–246.
16. Priya, A.K.; Yogeshwaran, V.; Rajendran, S.; Hoang, T.K.A.; Soto-Moscoco, M.; Ghfar, A.A.; Bathula, C. Investigation of mechanism of heavy metals ( $\text{Cr}^{6+}$ ,  $\text{Pb}^{2+}$  &  $\text{Zn}^{2+}$ ) adsorption from aqueous medium using rice husk ash: Kinetic and thermodynamic approach. *Chemosphere* **2022**, *286*, 131796.
17. Li, A.; Xie, H.; Qiu, Y.; Liu, L.; Lu, T.; Wang, W.; Qiu, G. Resource utilization of rice husk biomass: Preparation of MgO flake-modified biochar for simultaneous removal of heavy metals from aqueous solution and polluted soil. *Environ. Pollut.* **2022**, *310*, 119869. [[CrossRef](#)]
18. Tian, J.; Zhao, Z.H.; Kumar, A.; Boughton, R.I.; Liu, H. Recent progress in design, synthesis, and applications of one-dimensional  $\text{TiO}_2$  nanostructured surface heterostructures: A review. *Chem. Soc. Rev.* **2014**, *43*, 6920–6937. [[CrossRef](#)]
19. Liu, X.Y.; Steven, M.Z.; Liu, G.Q.; Li, Y.Q.; Zhang, R.H. Pretreatment of wheat straw with potassium hydroxide for increasing enzymatic and microbial degradability. *Bioresour. Technol.* **2015**, *185*, 150–157. [[CrossRef](#)]
20. Ye, E.; Regulacio, M.D.; Bharathi, M.S.; Pan, H.; Lin, M.; Bosman, M.; Win, K.Y.; Ramanarayan, H.; Zhang, S.Y.; Loh, X.J.; et al. An experimental and theoretical investigation of the anisotropic branching in gold nanocrosses. *Nano* **2016**, *8*, 543–552. [[CrossRef](#)]
21. Huang, K.; Dou, Q.; Loh, X.J. Nanomaterial mediated optogenetics: Opportunities and challenges. *RSC Adv.* **2016**, *6*, 60896–60906. [[CrossRef](#)]
22. Li, Z.; Ye, E.; Lakshminarayanan, D.R.; Loh, X.J. Recent advances of using hybrid nanocarriers in remotely controlled therapeutic delivery. *Small* **2016**, *12*, 4782–4806. [[CrossRef](#)] [[PubMed](#)]
23. Liu, S.; Sun, X.; Li, J.G.; Li, X.; Xiu, Z.; Yang, H.; Xue, X. Fluorine-and iron-modified hierarchical anatase microsphere photocatalyst for water cleaning: Facile wet chemical synthesis and wavelength-sensitive photocatalytic reactivity. *Langmuir* **2009**, *26*, 4546–4553. [[CrossRef](#)] [[PubMed](#)]
24. Renwick, L.C.; Brown, D.; Clouter, A.; Donaldson, K. Increased inflammation and altered macrophage chemotactic responses caused by two ultrafine particle types. *Occup. Environ. Med.* **2004**, *61*, 442–447. [[CrossRef](#)] [[PubMed](#)]
25. Alosaimi, E.H.; Alsohaimi, I.H.; Dahan, T.E.; Chen, Q.; Younes, A.A.; El-Gammal, B.; Melhi, S. Photocatalytic degradation of methylene blue and antibacterial activity of mesoporous  $\text{TiO}_2$ -SBA-15 nanocomposite based on rice husk. *Adsorp. Sci. Technol.* **2021**, *1*, 9290644. [[CrossRef](#)]
26. Wang, W.; Hu, C.; Fang, J.J.; Min, L. Large-scale preparation of rice-husk-derived mesoporous  $\text{SiO}_2@ \text{TiO}_2$  as efficient and promising photocatalysts for organic contaminants degradation. *Appl. Surf. Sci.* **2019**, *467*, 1187–1194. [[CrossRef](#)]
27. Adrian, C.M.L.; Suzana, Y.; Man, K.L.; Bridgid, L.F.C.; Muhammad, S.; Ayaka, Y.; Menandro, N.A. The effect of industrial waste coal bottom ash as catalyst in catalytic pyrolysis of rice husk for syngas production. *Energy Convers. Manag.* **2018**, *165*, 541–554.
28. Fatimah, I.; Said, A.; Hasanah, U.A. Preparation of  $\text{TiO}_2$ - $\text{SiO}_2$  using rice husk ash as silica source and the kinetics study as photocatalyst in methyl violet decolorization. *Bull. Chem. React. Eng. Catal.* **2015**, *10*, 43–49. [[CrossRef](#)]
29. Faiz, M.A.; Azurahaman, C.C.; Yazid, Y.; Suriani, A.B.; Ain, M.S.N. Preparation and characterization of graphene oxide from tea waste and its photocatalytic application of  $\text{TiO}_2$ /graphene nanocomposite. *Mater. Res. Express* **2020**, *7*, 015613. [[CrossRef](#)]